Adding Turbulence Based on Low-Resolution Cascade Ratios

Masato Ishimuroya[(✉)] and Takashi Kanai

The University of Tokyo, Graduate School of Arts and Sciences, Tokyo, Japan
`muroya@graco.c.u-tokyo.ac.jp`

Abstract. In this paper we propose a novel method of adding turbulence to low-res. smoke simulation. We consider the physical properties of such low-res. simulation and add turbulence only to the appropriate position where the value of the energy cascade ratio is judged as physically correct. Our method can prevent noise in the whole region of fluid surfaces which appeared with previous methods. We also demonstrate that our method can be combined with a variety of existing methods such as wavelet turbulence and vorticity confinement.

1 Introduction

In grid-based fluid simulation, when the number of grid cells is large, the computational time drastically increases while more highly detailed flulds with small eddies are obtained. Therefore, various methods for procedually adding turbulence (or up-scaling resolutions) have been proposed to obtain detailed fluid appearances from low-res. simulation results. Generally, the resulting fluid motion of low-res. simulation added with high-frequency turbulences is totally different from that of naïve high-res. simulation, because information on high-frequency components in low-res. simulation is completely lost due to the Nyquist limit and numerical dissipation. On the other hand, the addition of turbulence is still an efficient approach for CG animation since the visual quality is often preferred over the numerical precision.

A serious issue with previous methods for adding turbulence is that the results are too noisy in appearance due to the distribution of small eddies to the whole surface of fluid. One reason is that these methods do not consider the physical properties of turbulence in low-res. simulation, and consequently noises are uniformly added to the whole region of a vector field.

In this paper, we consider such physical properties when adding turbulences during the fluid simulation for smoke. We specifically calculate the energy cascade ratio in the spatial frequency domain from the results of low-res. simulation. We then add a noise and an eddie to only the appropriate position where the value of such a ratio is judged as physically correct. Since we use only one parameter for this addition, the amount of detail can easily be controlled and thus the design process of fluid animation can be simplified. Our method for evaluating the energy cascade is easy to implement and can be combined with a variety of existing methods for adding turbulence.

2 Related Work

In grid-based fluid simulation, Lots of adding turbulence methods have been proposed. We focus on two types of methods: One introduces eddies without changing the grid resolution, and the other adds high-frequency details by increasing the grid resolution.

In the former approach, Vorticity Confinement [1] introduces external forces that produce eddies into simulated fluid velocities. This method generates fine details that cannot be produced by the original simulation and can be applied not only for smoke simulation but also for water and explosion simulations using vortex particles [2]. However, the result looks too noisy due to the addition of eddies to the whole surface of fluid uniformly.

The latter approach is called up-resolution. This can inject highly detailed eddies which exceed the Nyquist frequency from low-resolution grids. Wavelet Turbulence [3] is a major method for this approach, which uses noise function and synthesizes high frequency noises to a coarse velocity field based on Kolmogorov's five-thirds law [4]. However, as for appearance performance, the result of adding turbulence is sometimes too noisy. The application of noise synthesis to liquid simulation [5], and a method for generating noises which have arbitrary spectral ratio and variance [6] have been proposed. All of these methods, however, do not consider the energy cascade of low-res simulation and still make the results noisy in appearance. To reduce the noisy appearance, an up-resolution approach based on data-driven techniques was proposed in [7]. This method applies the principal components analysis of coarse velocity field.

3 Our Approach

Our method for adding turbulence utilizes the physical property of turbulence, and the frequency ratio of the kinetic energy cascade from low-res simulation. By using this property, our method is able to add highly detailed noises or eddies.

We use the following notation in this paper. Non-bold italic characters denote scalars, such as n, k, and w. Bold characters denote a vector, such as $\mathbf{u}$ and $\mathbf{x}$. We attach a hat to denote a spectral component such as $\hat{\mathbf{u}}(\mathbf{x}, k)$. The common symbols used in this paper are shown in Table 1.

3.1 Kolmogorov's law

In general, when a fluid flow rises vertically, the flow is first a simple laminar flow, and as time passes, large eddies collapse and change into small eddies, and then the flow becomes complex turbulences. In the spatial frequency domain, laminar flow has low frequency and turbulence has a higher one. **Energy cascade** is the relationship of energy between larger eddies and smaller eddies in frequency. More properties of typical turbulent flows are described in [8]. For a position $\mathbf{x}$ and a spectral band k, the kinetic energy e is calculated by,

$$\hat{e}(\mathbf{x}, k) = \frac{1}{2}|\hat{\mathbf{u}}(\mathbf{x}, k)|^2. \tag{1}$$

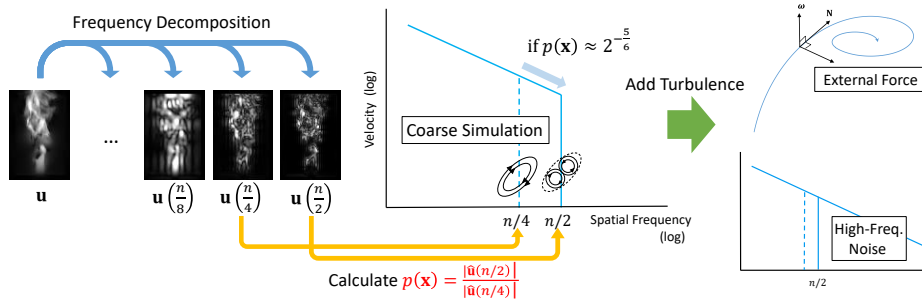| Variable (Resolution)	Symbol (Low)	(High)
Number of cells	n^3	N^3
Velocity	$\mathbf{u}$	$\mathbf{U}$
Position	$\mathbf{x}$	$\mathbf{X}$
Frequency band	k	
Kinetic energy	e	
Cascade ratio	p	

Table 1. Common symbols used in this paper.

Fig. 1. Our algorithm overview. In low-res simulation on n^3 grid, eddies up to $\frac{n}{2}$ frequency can be represented. If the cascade ratio follows Kolmogorov's law $2^{-\frac{6}{5}}$, high-frequency noise or external forces to inject turbulences are synthesized.

In turbulence, the kinetic energy follows Kolmogorov's five-thirds law [4],

$$\hat{e}(k) = C\epsilon^{\frac{2}{3}}k^{-\frac{5}{3}}, \tag{2}$$

where C is a constant and ϵ is the dissipation rate.

3.2 Overview

Our algorithm consists of the following steps:

1. Compute the ratio of energy cascade (called **cascade ratio** hereafter) for each cell in low-res grid.
2. Compare cascade ratio and Kolmogorov's five-thirds law.
3. For each cell, apply the procedure of adding turbulence in the original method only if the cascade ratio follows the law.

The above method adds the turbulence to the appropriate positions of the velocity grid, thereby alleviating the noisy appearance of fluid.

3.3 Evaluation of Energy Cascade

Calculating Cascade Ratio. To evaluate the cascade ratio, we perform frequency decomposition of velocity field. According to Eqs. (1) and (2), the velocity ratio between frequency components for band k and $2k$ can be expressed by,

$$\frac{|\hat{\mathbf{u}}(2k)|}{|\hat{\mathbf{u}}(k)|} = \frac{\sqrt{2\hat{e}(2k)}}{\sqrt{2\hat{e}(k)}} = \sqrt{2^{-\frac{5}{3}}} = 2^{-\frac{5}{6}}. \tag{3}$$

In a low-res grid with n^3 cells, the kinetic energy of flows which are developed and changed to turbulence should satisfy the following equation,

$$\frac{|\hat{\mathbf{u}}(\frac{n}{2})|}{|\hat{\mathbf{u}}(\frac{n}{4})|} = 2^{-\frac{5}{6}} \approx 0.56123. \tag{4}$$

We now define such a ratio $|\hat{\mathbf{u}}(n/2)|/|\hat{\mathbf{u}}(n/4)|$ as cascade ratio $p(n)$.

In our method, we decompose the low-res velocity field by using Wavelet Noise [9]. We then obtain two frequency components of velocity $\mathbf{u}$, $\hat{\mathbf{u}}(\frac{n}{2})$ in frequency band $[\frac{n}{4}, \frac{n}{2})$ and $\hat{\mathbf{u}}(\frac{n}{4})$ in $[\frac{n}{8}, \frac{n}{4})$. For each cell in the low-res grid, we calculate the ratio of their magnitudes from $\hat{\mathbf{u}}(\frac{n}{2})$ and $\hat{\mathbf{u}}(\frac{n}{4})$,

$$p(\mathbf{x}, n) = \frac{|\hat{\mathbf{u}}(\mathbf{x}, \frac{n}{2})|}{|\hat{\mathbf{u}}(\mathbf{x}, \frac{n}{4})|}. \tag{5}$$

From Eq. (4), we can say that if the velocity at position $\mathbf{x}$ contains turbulence, $p(\mathbf{x})/2^{-\frac{5}{6}} \approx 1$ is satisfied.

We now introduce a new function $s(\mathbf{x})$ in order to check whether the flow at position $\mathbf{x}$ is turbulence or not. The value of $s(\mathbf{x})$ can be determined by,

$$s(\mathbf{x}) = \begin{cases} 1 & \text{if} \quad 1 - \alpha < p(\mathbf{x})/2^{-\frac{5}{6}} < 1 + \alpha, \\ 0 & \text{otherwise,} \end{cases} \tag{6}$$

where α is a positive value specified by the user. We apply this function s to the two methods, Wavelet Turbulence and Vorticity Confinement respectively.

Determining α. With our approach, we determine α by using one of the following,

- a value fixed by the user,
- a value which changed dynamically in each grid, depending on the magnitude of its velocity.

The latter is based on Reynolds number, which means that the occurrence probability of turbulence is proportional to the flow speed. Generally, as the Reynolds number becomes higher, the flow tends to be more turbulent. If we set parameters except the flow speed constant values, Reynolds number becomes proportional to the flow speed. Thus α can be determined by,

$$\alpha = \alpha' \frac{|\mathbf{u}(\mathbf{x})|}{|\bar{\mathbf{u}}|}, \tag{7}$$

where α' is a value fixed by the user, and $\overline{\mathbf{u}}$ is the average velocity in the scene. Because the value of α can affect the amount of turbulence, finding appropriate α for user desired results by trial and error is needed, According to the experiments, we found that $0.1 \leq \alpha \leq 0.2$ is good for suitable turbulence.

3.4 Application to Wavelet Turbulence

For Wavelet Turbulence, we create 3D noise textures in several different frequency bands by Wavelet Noise [9], and synthesize them to low-res velocity field with weighting for each band based on Eq. (2) like Perlin Noise [10]. In this method, the high frequency noise $\mathbf{y}(\mathbf{x})$ is defined by,

$$\mathbf{y}(\mathbf{x}) = \sum_{i=i_{min}}^{i_{max}} \mathbf{w}(2^i \mathbf{x}) 2^{-\frac{5}{6}(i-i_{min})}, \tag{8}$$

where $\mathbf{w}(\mathbf{x})$ is the curl of a noise texture which is divergence-free [11], and $(i_{min}, i_{max}) = (\log n, \log \frac{N}{2})$. The other variables are shown in Table 1. High frequency noise $\mathbf{y}$ is thought to be a cascade from the result of low-res simulation. Therefore, by weighting $\mathbf{y}(\mathbf{x})$ with the frequency component of kinetic energy e for band $n/2$, the velocity $\mathbf{U}$ in high-res grid is calculated by,

$$\mathbf{U}(\mathbf{X}) = \mathtt{Lerp}(\mathbf{u}, \mathbf{X}) + 2^{-\frac{5}{6}} \mathtt{Lerp}\left(\hat{e}\left(\mathbf{x}, \frac{n}{2}\right), \mathbf{X}\right) \mathbf{y}(\mathbf{X}), \tag{9}$$

where $\mathtt{Lerp}$ is the linear interpolation operator for up-samplling. $\mathtt{Lerp}(\mathbf{u}, \mathbf{X})$ and $\mathtt{Lerp}(\hat{e}, \mathbf{X})$ are vector and scalar fields by linear interpolation from low resolution field $\mathbf{u}(\mathbf{x})$ and $\hat{e}(\mathbf{x})$ respectively to high resolution grid $\mathbf{X}$. The first term of the right side in Eq. (9), $\mathtt{Lerp}(\mathbf{u}, \mathbf{X})$, is a simple mapping linearly interpolated from a coarse velocity field, and the second term is that of higher frequency eddies. With our approach, we consider not only the weight $\hat{e}(\mathbf{x}, n/2)$ but also the cascade ratio $p(\mathbf{x}, n)$. For this reason, we integrate the function $s(\mathbf{x})$ into Eq. (9),

$$\mathbf{U}(\mathbf{X}) = \mathtt{Lerp}(\mathbf{u}, \mathbf{X}) + 2^{-\frac{5}{6}} \mathtt{Lerp}(s(\mathbf{x}), \mathbf{X}) \mathtt{Lerp}\left(\hat{e}\left(\mathbf{x}, \frac{n}{2}\right), \mathbf{X}\right) \mathbf{y}(\mathbf{X}). \tag{10}$$

According to Eq. (10), if the ratio follows Kolmogorov's law, we determine the flow to be turbulence and synthesize the noise texture based on the law (see Fig. 1). Otherwise, we simply apply linear interpolation to a low-res velocity field. Although noise field $\mathbf{y}$ is incompressible, the velocity field after synthesizing the noise violates incompressibility. This is because the weight of $\mathbf{y}$ differs depending on position $\mathbf{x}$, and this problem occurs at Eq. (9). However, the noise is small enough in magnitude and high frequency. Thus, it can be assumed that influence of compressibility is negligible in appearance.

We set $\mathbf{c}(\mathbf{x}) = (c_u(\mathbf{x}), c_v(\mathbf{x}), c_w(\mathbf{x}))$ for a set of texture coordinates. By advecting $\mathbf{c}(\mathbf{x})$ along with the low-res velocity field, the noise turbulence appears to advect with the flow.

3.5 Application to Vorticity Confinement

We also apply our method to Vorticity Confinement in low-res fluid simulation. For each frame of the simulation, we compute the cascade ratio from original simulation. In only places where the ratio follows the law, we add external forces to produce eddies. Our algorithm is shown in Algorithm 1. The difference between the previous method and ours is highlighted in red.

Algorithm 1 Vorticity confinement in consideration to the cascade ratio

---

1: Calculate $\mathbf{u}^n$, the fluid velocity at frame n
2: Vorticity $\boldsymbol{\omega} = \nabla \times \mathbf{u}^n$, $N = \frac{\nabla|\boldsymbol{\omega}|}{|\nabla|\boldsymbol{\omega}||}$
3: Calculate $s(\mathbf{x})$ from $\mathbf{u}^n$
4: $\mathbf{f}'_{vort} = \varepsilon h s(\mathbf{x}) \left(N \times \boldsymbol{\omega} \right)$
5: $\mathbf{u}^{n+\frac{1}{2}} = \mathbf{u}^n + \mathbf{f}'_{vort}$
6: $\mathbf{u}^{n+1} = \mathbf{u}^{n+\frac{1}{2}} + \mathbf{f}_{ext} - (\mathbf{u} \cdot \nabla)\mathbf{u} + \frac{1}{\rho}\nabla p - \nu\nabla^2\mathbf{u}$

Unlike the application to Wavelet Turbulence, this method cannot limit the frequency of eddies. So it does not guarantee that only high frequency eddies will be added. Although the behavior of flows can be drastically changed compared to that before adding eddies, this issue happens when simulating with low-res grid and we can modify the behavior in a short time. As for incompressibility, the velocity field can be kept divergence-free because we perform pressure projection after adding eddies. Since we add external forces only to turbulent flows, uniform noisy appearance can be alleviated.

4 Results and Discussion

Figs. 2 and 3 show the results of up-resolution by Wavelet Turbulence and our method in a $48 \times 64 \times 48$ low-res grid. We implement our method and for comparison based on the source code of Wavelet Turbulence [12]. For low-res velocity fields, we simulated a smoke plume by heat buoyancy and we use the standard simulation framework proposed in [13] and MacCormack method [14] for advection. In our implementation, when computing a cascade ratio $p(\mathbf{x})$ we use the mean value of $|\hat{\mathbf{u}}(\mathbf{x}, k)|$ at a cell including position $\mathbf{x}$ and its surrounding cells instead of the frequency component only at a cell of $\mathbf{x}$. Figs. 2 and 3 show the results of the 70th, 120th frames, respectively. In the result of the previous method (b), too much small noises appear compared to low-res simulation (a) which is undesirable. (c) and (d) are the results of our method. Compared to the original Wavelet Turbulence result (b), our method can synthesize noises to prevent the shape of smoke from changing in low-res simulation. In addition, compared to (b) in which high-frequency noises appear even in laminar flows on the lower part of fluid, such noises do not appear on the lower part of the fluid in our results (c) and (d). Fig. 4 is another result of up-resolution. We used
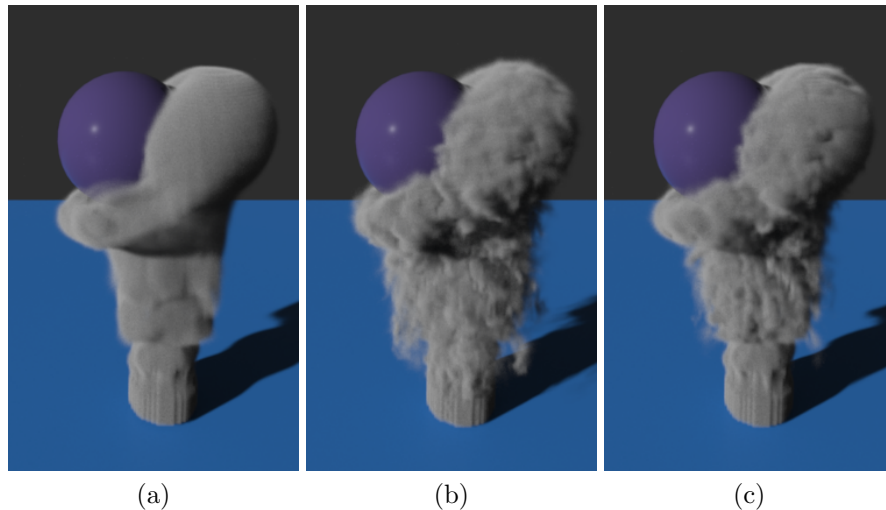
Fig. 2. Result of 70th frame for simulation of Fig. 1. (a) Linear interpolation. (b) Wavelet Turbulence. (c) Our method with $\alpha = 0.1$ everywhere.

the IVOCK scheme [15] for $48 \times 64 \times 48$ low-res. simulation. As seen from the results, the same can be said for Figs. 2 and 3. These results indicate that noisy appearance can be controlled by our method.

Fig. 5 shows simulation results using Vorticity Confinement with and without our cascade evaluation. It can be seen that larger eddies appear in our method. Fig. 6 is an quantitative evaluation of the results between the previous method and ours by using color map of cascade ratio $p(\mathbf{x})$. As a whole, the ratio in our method is closer to the ideal ratio of turbulence model than that in the previous method, which shows higher ratio (more high-frequency eddies) than the ideal one.

Limitation. By taking the contraposition of Eq. (4) logically, at positions where the cascade ratio is out of range from its standard value $2^{-\frac{5}{6}}$, the flow is not turbulence. However, in the actual simulation, the cascade ratio may be affected not only by the physical properties considered in this paper but also by numerical errors in frequency decompositions, especially numerical diffusion in advection. Therefore the cascade ratios we compute can be different from correct values. Currently, we cannot identify the cause of the cascade ratio being out of range, and we will address these issues in future work.

5 Conclusion and Future Work

In this paper, we have proposed a method to apply the ratio of kinetic energy cascade to two methods for adding turbulence in smoke simulation. Our method can improve noise appearance and can make it more natural.
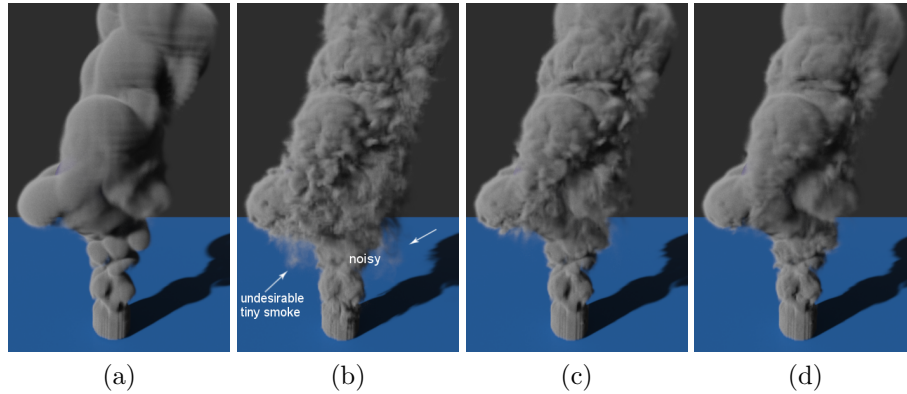
|(a)|(b)|(c)|(d)|

Fig. 3. Addition of turbulence for coarse grid simulations. The result of the 135th frame is shown. (a) Linear interpolation of coarse simulation. (b) Wavelet Turbulence. (c) Our method with $\alpha = 0.1$ everywhere. (d) Our method with α depending on the magnitude of velocity.

In future work, we hope to combine this cascade evaluation with other methods for adding turbulence and apply it to other types of fluids such as liquids.

References

1. Fedkiw, R., Stam, J., Jensen, H.W.: Visual simulation of smoke. In: Proc. SIG-GRAPH '01, ACM Press, New York (2001) 15–22
2. Selle, A., Rasmussen, N., Fedkiw, R.: A vortex particle method for smoke, water and explosions. ACM Trans. Graph. **24** (2005) 910–914
3. Kim, T., Thürey, N., James, D., Gross, M.: Wavelet turbulence for fluid simulation. ACM Trans. Graph. **27** (2008) 50:1–50:6
4. Kolmogorov, A.N.: The Local Structure of Turbulence in Incompressible Viscous Fluid for Very Large Reynolds' Numbers. In: Dokl. Akad. Nauk SSSR. Volume 30. (1941) 301–305
5. Narain, R., Sewall, J., Carlson, M., Lin, M.C.: Fast animation of turbulence using energy transport and procedural synthesis. ACM Trans. Graph. **27** (2008) 166:1–166:8
6. Zhao, Y., Yuan, Z., Chen, F.: Enhancing fluid animation with adaptive, controllable and intermittent turbulence. In: Proc. ACM SIGGRAPH/Eurographics Symposium on Computer Animation. (2010) 75–84
7. Sato, S., Morita, T., Dobashi, Y., Yamamoto, T.: A data-driven approach for synthesizing high-resolution animation of fire. In: Proceedings of the Digital Production Symposium. DigiPro '12, New York, NY, USA, ACM (2012) 37–42
8. Thuerey, N., Kim, T., Pfaff, T.: Turbulent fluids. In: ACM SIGGRAPH 2013 Courses. SIGGRAPH '13, New York, NY, USA, ACM (2013) 6:1–6:1
9. Cook, R.L., DeRose, T.: Wavelet noise. ACM Trans. Graph. **24** (2005) 803–811
10. Perlin, K.: An image synthesizer. In: Proceedings of the 12th Annual Conference on Computer Graphics and Interactive Techniques. SIGGRAPH '85, New York, NY, USA, ACM (1985) 287–296
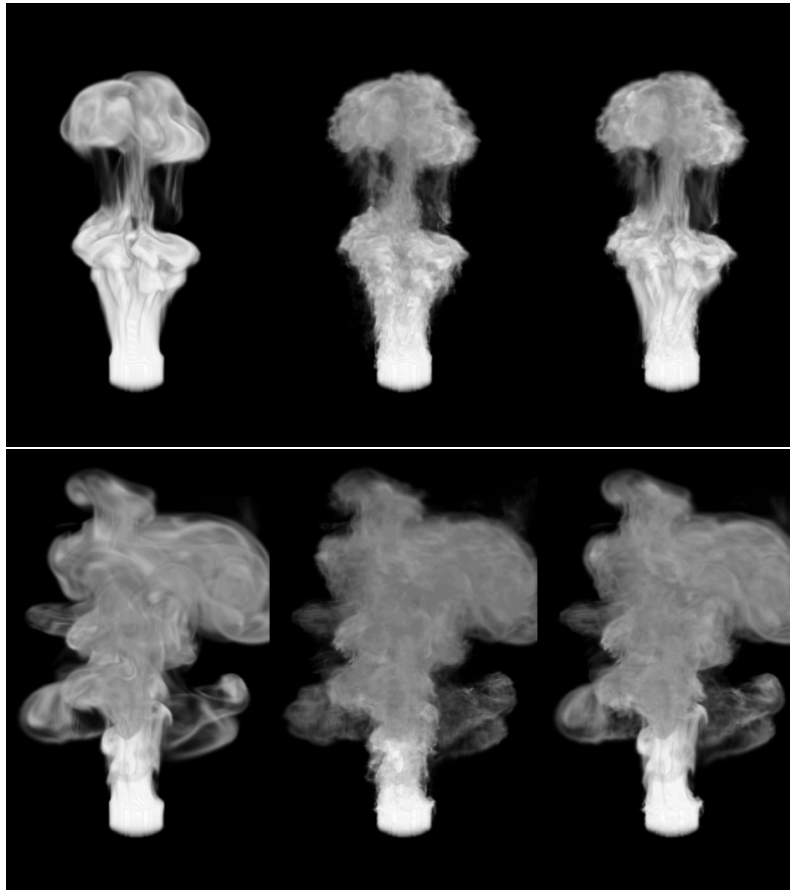
Fig. 4. Another result of smoke plume. Left: Linear interpolation. Middle: Wavelet Turbulence. Right: Our method with $\alpha = 0.2$ everywhere. The upper row is the result of the 104th frame and the lower is that for 231st frame.

11. Bridson, R., Houriham, J., Nordenstam, M.: Curl-noise for procedural fluid flow. In: ACM SIGGRAPH 2007 Papers. SIGGRAPH '07, New York, NY, USA, ACM (2007)
12. Kim, T., Thürey, N.: Wavelet turbulence source code. `http://www.cs.cornell.edu/~tedkim/wturb/source.html` (2008)
13. Stam, J.: Stable fluids. In: Proceedings of the 26th Annual Conference on Computer Graphics and Interactive Techniques. SIGGRAPH '99, New York, NY, USA, ACM Press/Addison-Wesley Publishing Co. (1999) 121–128
14. Selle, A., Fedkiw, R., Kim, B., Liu, Y., Rossignac, J.: An unconditionally stable maccormack method. J. Sci. Comput. **35** (2008) 350–371
15. Zhang, X., Bridson, R., Greif, C.: Restoring the missing vorticity in advection-projection fluid solvers. ACM Trans. Graph. **34** (2015) 52:1–52:8
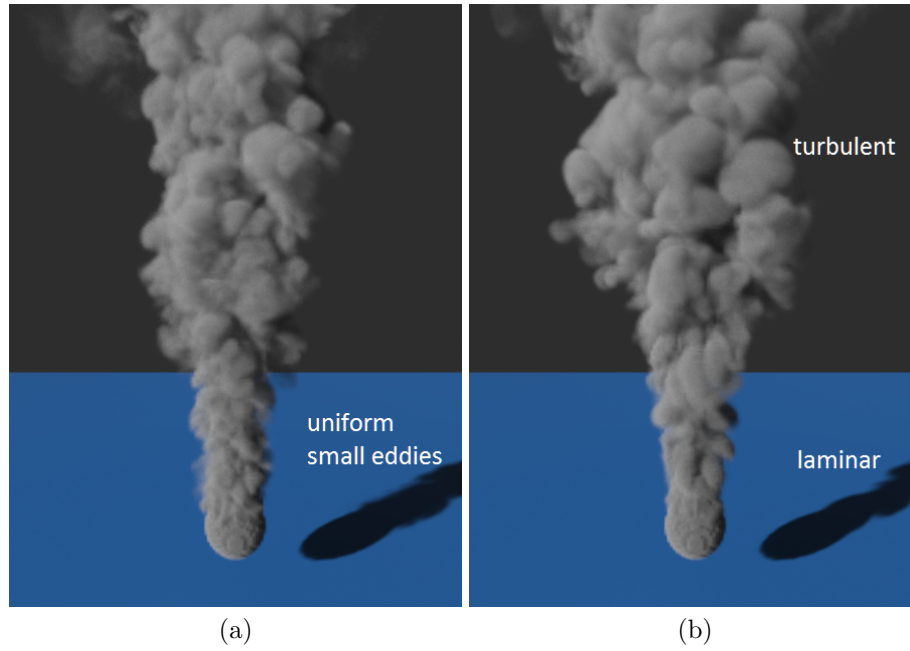
Fig. 5. (a) Vorticity Confinement. (b) Vorticity Confinement with our cascade evaluation.
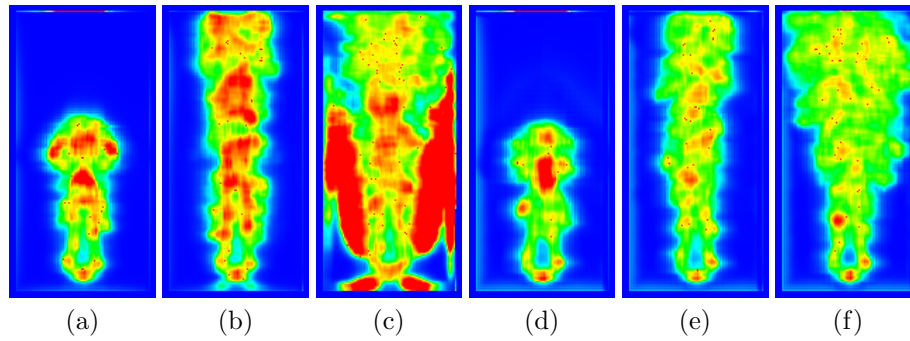

Fig. 6. Cascade ratios of Vorticity Confinement with and without our method. (a), (b) and (c) are the results of only Vorticity Confinement and (d), (e) and (f) are those from our method. In this figure, green pixels correspond to the ideal ratio of the turbulence model $p(\mathbf{x}) = 2^{-\frac{5}{6}}$, the red corresponds to higher ratios, and the blue to lower ones.